

Submitted: 01/12/2022

Accepted: 17/02/2023

Published: 25/03/2023

Histiocytic sarcoma with spinal necrosis in a dog with progressing non-ambulatory tetraparesis

Yuki Nemoto^{1*} , Munekazu Nakaichi² , Masashi Sakurai³ , Kazuhito Itamoto⁴ , Masahiro Morimoto³ , Hiro Horikirazono² , Harumichi Itoh⁴ , Hiroshi Sunahara¹  and Kenji Tani¹ 

¹Department of Veterinary Surgery, Joint Faculty of Veterinary Medicine, Yamaguchi University, Yamaguchi, Japan

²Department of Veterinary Radiology, Joint Faculty of Veterinary Medicine, Yamaguchi University, Yamaguchi, Japan

³Department of Veterinary Pathology, Joint Faculty of Veterinary Medicine, Yamaguchi University, Yamaguchi, Japan

⁴Department of Veterinary Small Animal Clinical Science, Joint Faculty of Veterinary Medicine, Yamaguchi University, Yamaguchi, Japan

Abstract

Background: Histiocytic sarcoma (HS) is an aggressive malignant neoplasm, and widespread metastasis occurs with a fatal outcome. HS involving the central nervous system is relatively uncommon. Spinal cord necrosis, a very rare condition, could be induced by ischemia or infarction. Here, we report a dog progressing non-ambulatory tetraparesis with spinal cord necrosis caused by HS.

Case Description: A 9-year-old male Labrador Retriever was presented with a progressing non-ambulatory tetraparesis. CT imaging revealed lysis of the spinous process of T7 and a ring-shaped lesion surrounding the soft tissue of lung fields. T2-weighted MRI showed the spinous processes of T6 to T8 as hyperintense, and the lesion infiltrated into the T7 vertebra and the spinal cord. After euthanasia, the final diagnosis upon necropsy was HS, which was observed in the lung, spinous process, thoracic cord, and the pulmonary hilar lymph node. Moreover, necrotic spots were spread widely through the thoracic spinal cord.

Conclusion: This report outlines a case of canine HS in the lung, spinous process, thoracic cord, and pulmonary hilar lymph node. Ischemic deficit and necrosis of the thoracic spinal cord resulted from the compression of perivascular tumor cells, which rapidly led to progressive tetraparesis. Although the diagnosis was difficult, MRI and CT images helped determine the prognosis. To our knowledge, this is the first case report of canine HS with direct spinal cord involvement associated with spinal necrosis.

Keywords: Dog, Histiocytic sarcoma, Spinal cord necrosis.

Introduction

Histiocytic sarcoma (HS) is an aggressive malignant neoplasm, and widespread metastasis occurs with a fatal outcome (Dervisis *et al.*, 2017). Canine HS has been mainly identified in middle-aged to older purebred dogs including Bernese mountain dogs, Retrievers and Rottweilers (Fulmer and Mauldin, 2007). Most canine HS arises from dendritic cells (Affolter and Moore, 2002). HS may occur as a localized disease or may involve dissemination, with the involvement of several organs. Localized HS is invasive locally, but it can metastasize to multiple organs, including the spleen, lungs, liver, bone marrow, subcutaneous tissue, bones, skeletal muscles, kidneys, and central nervous system (CNS). Treatment with surgery, chemotherapy, radiation, and a combination of these have suggested improved outcome, however, the prognosis is still poor (Dervisis *et al.*, 2017). Canine HS involving CNS is

relatively uncommon, representing 2.2% of primary and 3.4% of secondary intracranial neoplasms diagnosed at necropsy (Song *et al.*, 2013). CNS HS is often characterized by severe inflammation (Tamura *et al.*, 2009; Song *et al.*, 2013; Mariani *et al.*, 2015; Ishikawa *et al.*, 2016; Thongtharb *et al.*, 2016; Wada *et al.*, 2017); however, reports are still limited.

Spinal cord necrosis, a rare condition, can be induced by ischemia or infarction (Yasui *et al.*, 2017; Ogawa *et al.*, 2019). In humans, this may happen in patients with vascular risk factors and who had aortic surgery, causing back pain, numbness, and motor weakness (Yasui *et al.*, 2017; Ogawa *et al.*, 2019). In dogs, there have been no reports except for spinal cord injuries, which directly damage the spinal cord. Here, we report a dog progressing non-ambulatory tetraparesis with spinal cord necrosis, in which the HS was observed in the lung, spinous process, thoracic cord, and the pulmonary hilar lymph node.

*Corresponding Author: Yuki Nemoto. Department of Veterinary Surgery, Joint Faculty of Veterinary Medicine, Yamaguchi University, Yamaguchi, Japan. Email: y.nemoto@yamaguchi-u.ac.jp.

Case Details

A 9-year-old male Labrador Retriever was referred to the Yamaguchi University Animal Medical Center with a progressing non-ambulatory tetraparesis. Pelvic ataxia was present 12 days before referral, followed by dysuria and tetraparesis 9 days before referral. On presentation, the dog showed aggressive behavior with panting with stretching thoracic limbs and no movement in either pelvic limb. Physical parameters were within normal limits, except for a body temperature of 39.9°C. On palpitation of the cervical spine, hyperesthesia was detected. The dorsal part was not examined because of the dog's aggressive behavior. The flexor withdrawal reflexes were normal for both thoracic and pelvic limbs. On neurological examination, a lesion was localized to the C1–C5 spinal cord segments, but C6–T2 segments could not be excluded because of progressive tetraparesis from the pelvic limbs to the thoracic limbs. A complete blood cell count revealed neutrophilia with left shift ($304.3 \times 10^2/\mu\text{l}$; reference range: 19.25–146.25 $\times 10^2/\mu\text{l}$) and monocytosis ($47.4 \times 10^2/\mu\text{l}$; reference range: 3.0–10.0 $\times 10^2/\mu\text{l}$). The chemistry profile detected high creatine phosphokinase (263 IU/l; reference range: 49–166 IU/l) and high C-reactive protein (2.9 mg/dl; reference range: <1.0 mg/dl). Other comprehensive metabolic panels showed normal results. Thoracic radiographs detected bone lysis of the T7 spinous process and an approximately 1 cm high signal-intensity ring-shaped lesion in the lung (Fig. 1A and B). Urinalysis and fecal examination did not reveal any significant changes. Differential diagnoses included inflammation caused by systemic mycosis and/or bacterial infection and neoplasia. Computed tomography (CT) and magnetic resonance imaging (MRI) were conducted under general anesthesia.

CT images revealed bone lysis of spinous processes of T7 and T8. Enhanced media detected homogenous contrast around the spinous processes and vertebral body of T7 (Fig. 2A). A ring-shaped lesion surrounding the soft tissue of the lung fields was detected as the same as an X-ray in the right cranial lobe (Fig. 2B). On the T1-weighted MRI, strong homogenous contrast enhancement highlighted post-contrast sequences at the lesion of T7 spinous process. A slight enhancement was observed in the middle of the vertebral body of T7 (Fig. 3A and B). On T2-weighted MRI, the spinous processes of T6 to T8 were hyperintense, and the lesion infiltrated into the vertebral body of T7 and spinal cord (Fig. 3C). Specific abnormalities were not detected for the cervical part by either CT or MRI. With examinations on the first day, neither infection nor neoplasm could be identified. The dog was hospitalized at the owner's request. Antibiotics, including Vibramycin (7 mg/kg BID, p.o) and clarithromycin (8.9 mg/kg BID, p.o), were given during the hospitalization.

Bronchoalveolar lavage (BAL), cerebrospinal fluid (CSF) collection, and the biopsy of T7 were performed under anesthesia 5 days following referral. Bronchoscopy showed a polyp with small capillary vessels, but sputum was not detected. The polyp was taken for pathological examination. With BAL, neither tumor cells nor bacteria were detected. White blood cells in the CSF obtained from the cerebellomedullary cistern were 17 μl (normal reference range <5 μl). CSF specific gravity was 1.006 (normal reference range: 1.005–1.007). A biopsy of T7 was performed by making an incision from the dorsal side. Necrotic tissue was located between the spinous process and muscle. These tissues were taken with forceps. Histology of the polyp showed hydropic degeneration, but neither

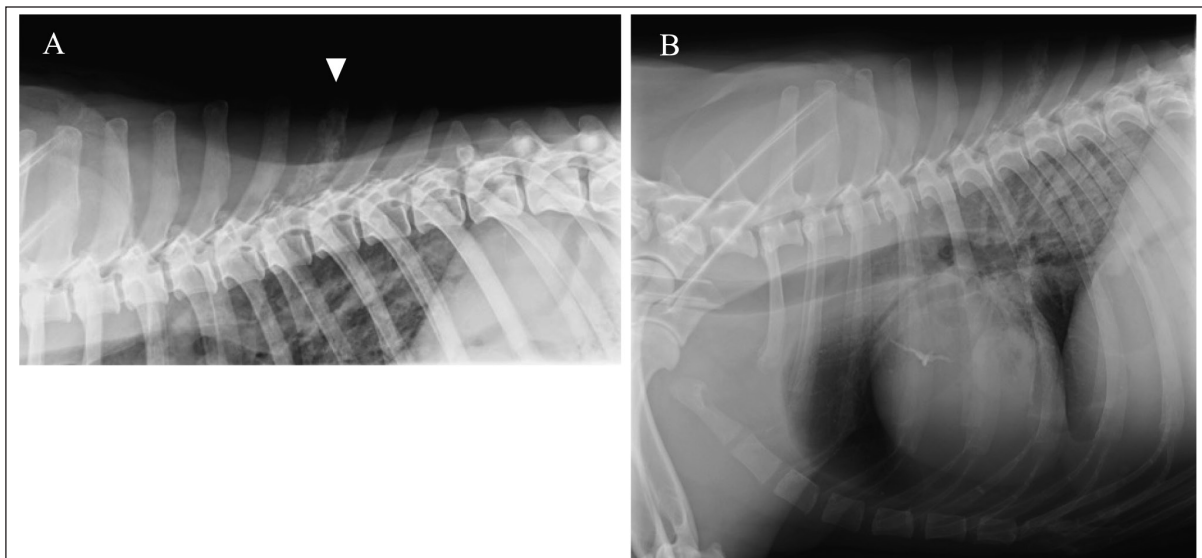


Fig. 1. Right lateral thoracic radiograph. Bone lysis of T7 spinous process (A). Approximately 1-cm high signal-intensity ring-shaped lesion in the lung (B).

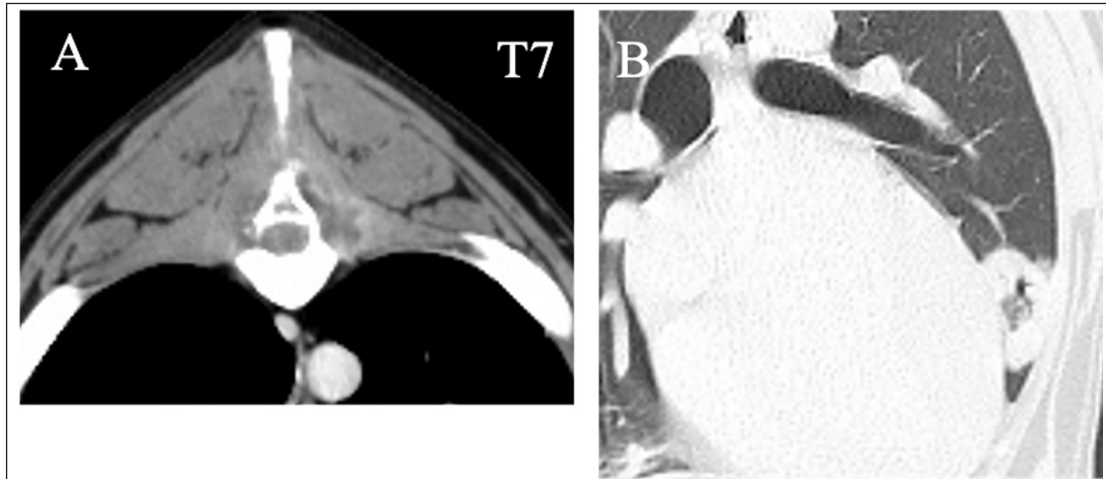


Fig. 2. Transverse contrast CT images show the lysis of the spinous process of T7 (A). Enhanced media detected homogenous contrast around the spinous processes and the T7 vertebra. Transverse CT images show the round, thin-walled cavity in the right cranial lobe of lung fields (B).

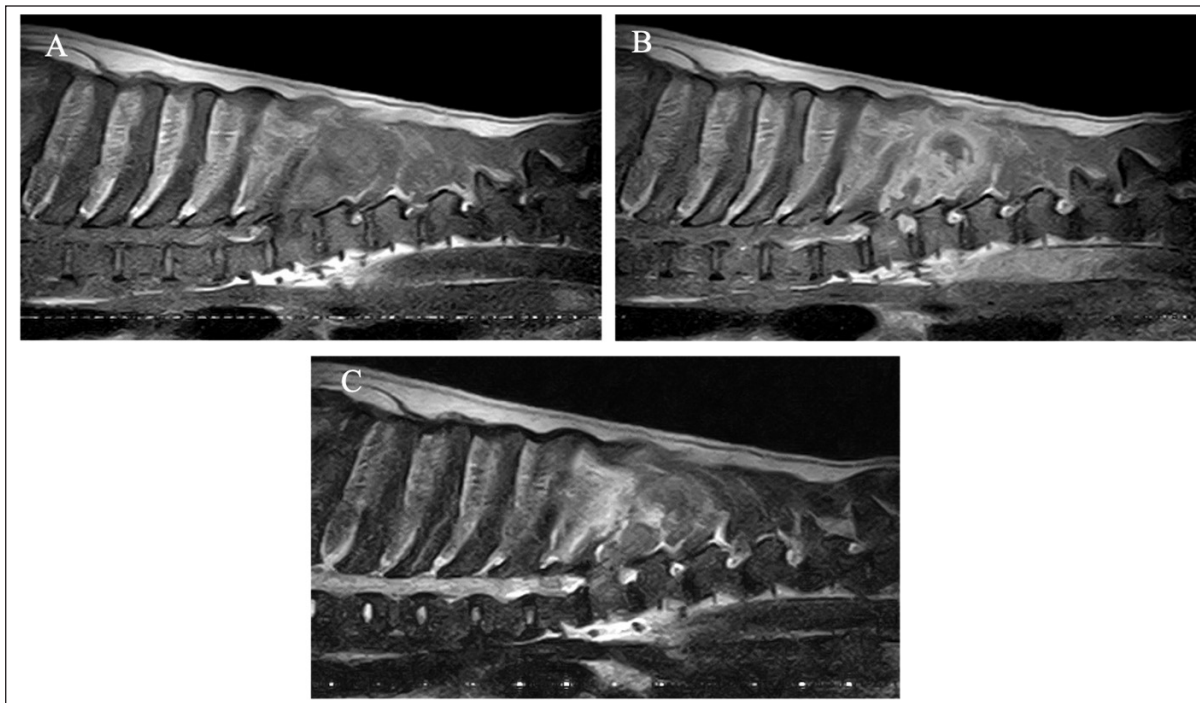


Fig. 3. MRI images in the sagittal plane. On T1-weighted images without (A) and with (B) contrast. Strong homogenous contrast enhancement is observed in post-contrast sequences at the lesion of the T7 spinous process. Slight enhancement is observed in the middle of the T7 vertebra. On T2-weighted images, the spinous processes of T6 to T8 are hyperintense, and the lesion infiltrated into the spinal cord and the T7 vertebra (C).

neoplasia nor inflammation was observed. For T7, no neoplasm or bacterial, fungal lesion was observed, but fibrous and necrotic tissue growth was seen. No organisms were found by histopathology, including hematoxylin and eosin, periodic acid-Schiff, Ziehl-Neelsen, and Gram staining. The dog was euthanized

at the owner's request on the next examination day. No bacteria (anaerobic or aerobic) or fungus were detected from the blood and urine taken during the first visitation.

During the necropsy of the right lung lobe, multiple white-yellowish masses (up to 5 cm in diameter) were

found, and the cranial lobe had a yellowish ring-shaped lesion ($2.7 \times 3.5 \times 1.5$ cm, with a 1.0-cm normal area in the center). No pus leaked from the cut surface of the lung. The pulmonary hilar lymph node was mildly enlarged. T7 spinous process became fragile. On the right side of the T7 spinous process, a yellowish mass (3 cm in diameter) was attached. Although the surface of the spinal cord was normal, dark brown spots and small cavitation were scattered in the transverse section of the T1–12 spinal cord.

Histopathological examination revealed diffuse and invasive growth of large oval neoplastic cells in pulmonary lesions. The large neoplastic cells had an abundant, occasionally vacuolated cytoplasm (Fig. 4A). The mitotic index was 12 in 10 high-power fields. The frequent observation of giant nuclei indicated severe atypia. CD3-positive T lymphocytes infiltrated around the tumor cells. Immunohistochemically, large neoplastic cells were positive for ionized calcium-binding adapter molecule 1 (Iba1), a highly sensitive marker of histiocytic cells (Fig. 4B). Numerous Ki67-positive proliferating cells were found, and Ki67 index was 20.6% (Fig. 4C). Histopathology revealed tumor

tissue of the same origin in the T7 spinous process and pulmonary hilar lymph node mass lesion. In addition, diffuse necrosis was found through the thoracic cord (T1–T13). The perivascular proliferation of tumor cells was found in the remaining thoracic spinal cord tissue (Fig. 4D), and these round cells contained Iba1-positive histiocytic tumor cells. Based on these findings, we diagnosed HS in the lung and its metastasis to the pulmonary hilar lymph node, T7, and thoracic spinal cord, which had lymphocytic infiltration.

Discussion

Here, we report pulmonary HS caused necrosis of the spinal cord in a dog. In primary pulmonary HS, the distribution of lesions has been reported mainly in the liver, spleen, and abdominal lymph nodes (Fulmer and Mauldin, 2007; Yasui *et al.*, 2017). A few cases have been reported to involve the bones but not the nervous system. In our case, pulmonary HS affected the lung, spinal cord, spinous process, and lymph node. Clinically, rapid progress to non-ambulatory tetraparesis was observed. A direct cause of tetraparesis could be the necrosis of the thoracic spinal cord.

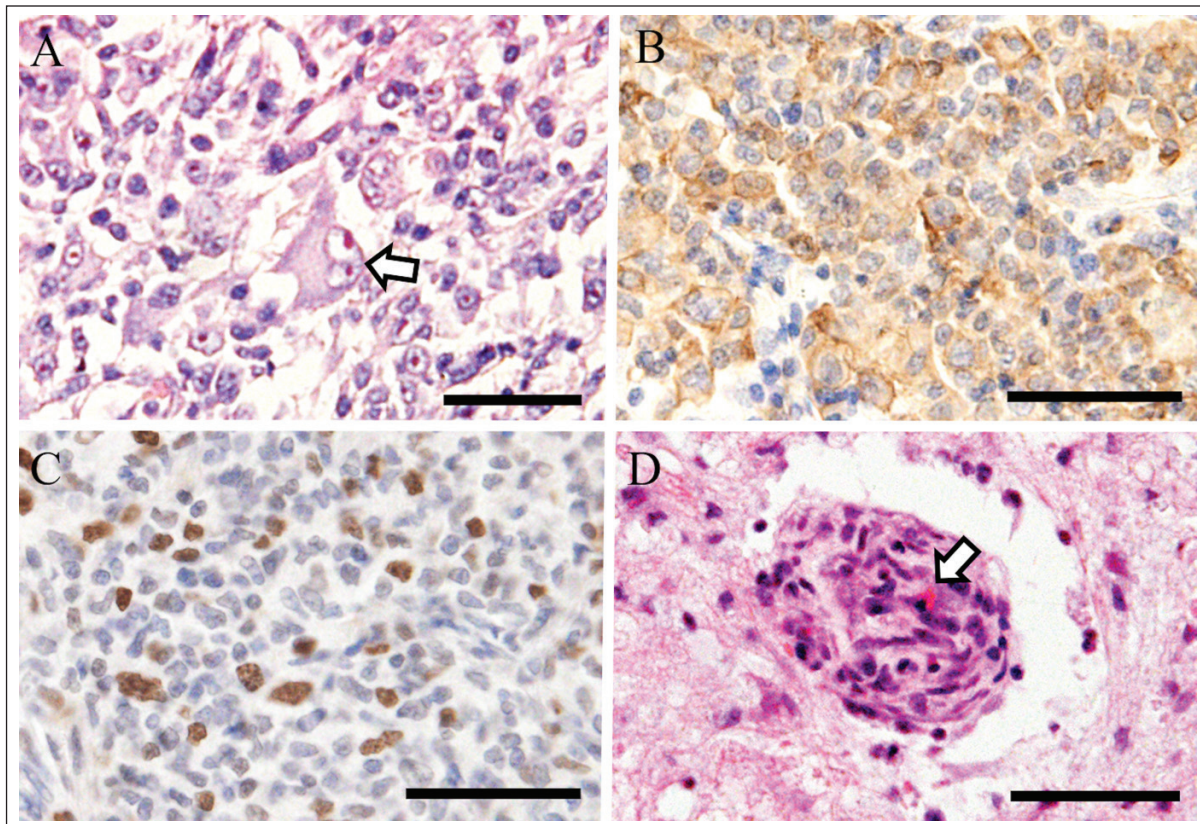


Fig. 4. Histopathology of tumor in the lung (A–C) and spinal cord (D). Neoplastic cells have an abundant round cytoplasm. A giant nucleus indicated severe atypia (arrow) (A). Immunohistochemically, neoplastic cells are positive for Iba1 (B). Ki67-positive proliferating cells are numerous (C). Perivascular tumor proliferation compresses blood vessel (arrow) in the thoracic spinal cord (D). Hematoxylin and eosin stain (A, D). Immunohistochemistry with hematoxylin counterstain (B, C). All photographs were captured at magnification of 400x. Bars are 50 μ m (A–D).

Ischemic deficit might happen owing to the compression of the perivascular tumor cells. Spinal cord necrosis is an uncommon event and is generally caused by spinal cord ischemia or infarction. Infarction of the cervical cord may present with pain, paralysis, dissociated sensory loss, and autonomic deficit (Yasui *et al.*, 2017; Ogawa *et al.*, 2019). In humans, it is mainly caused by dissociation of the ascending aorta as a complication after aortic surgery (Yasui *et al.*, 2017). Spinal tumor metastasis can also cause neuropathy by spinal cord compression, but only spinal epidural metastasis and lung cancer have been reported (Yasui *et al.*, 2017). The process of spinal cord ischemia was reported to include the tumor reaching the spinal cord indirectly via an initial hematogenous spread to the vertebral body, followed by growth in the bone and spread into the epidural space, eventually causing secondary compression of the spinal cord. A direct invasion of a paravertebral tumor into the spinal canal through an intervertebral foramen, which compresses the spinal cord, is less common. In this case, this widespread necrosis could happen because of the compression of the vessel by the perivascular proliferation of tumor cells, and the metastasis of the spinal cord was also involved. With the process of tumor invasion, inflammation occurred as indicated by elevated creatine phosphokinase and C-reactive protein. In dogs, no reports of spinal necrosis caused by a tumor have been reported. The tumor involved in the spinal cord can compress the spinal artery and cause circulatory disorders. In our case, HS involved the lung, spinous process, and spinal cord, a pattern that we believe has never been reported previously.

The reported radiographic characteristics of pulmonary HS involve a large mass in the periphery of the whole lobe of the right middle or left cranial lung lobe with an internal air bronchogram (Toyoda *et al.*, 2020). X-ray images showed a solitary mass located in the left cranial lung lobe and lymphadenopathy similar to the findings reported previously (Toyoda *et al.*, 2020). However, the appearance of a ring-shaped lesion has not been reported in an HS case. The CT finding was interpreted as a reverse halo sign, i.e., a focal, rounded area of ground attenuation surrounded by a more or less complete ring of consolidation, which has been rarely reported in dogs (Secretst and Sakamoto, 2014). A previous report of four dogs with reverse halo signs showed neoplasia, lung lobe torsion, and abscess. In the neoplasia cases with a reverse halo sign, a rim of neoplastic cells with areas of necrosis and central hemorrhage, and preservation of alveolar and bronchiolar architecture were detected. In this case, necrosis or hemorrhage was not detected, but normal lung tissue was preserved with surrounding tissue of HS and lymphocytic infiltration. These observations suggest the possibility of a process of progression or inflammation, and necrosis or hemorrhage may be

detected at the end. To the best of our knowledge, this is the first report of HS with a reverse halo sign.

Some MRI reports of HS involving the CNS or spinal cord typically showed the neoplastic lesion as a diffuse parenchymal disease involving the spinal cord and meninges (Ogawa *et al.*, 2019), and some reported that multifocal mass lesions were detected (Taylor *et al.*, 2015). We did not observe these features in this case, and instead, there was remarkably extensive lysis of the spinous process, which was not observed previously. The anatomic structure of the spinous process was not mostly maintained, which was also detected with CT images. In this case, at the time, it was difficult to make a tentative diagnosis of metastasis of the lung tumor. However, the images made it clear that widespread inflammation occurred, which enabled us to predict the prognosis of this case. Considering the possibility of this prognosis could be helpful for both veterinarians and owners.

In conclusion, this report outlines a case of canine HS in the lung, spinous process, thoracic cord, and pulmonary hilar lymph node. The compression of perivascular tumor cells resulted in an ischemic deficit and necrosis of the thoracic spinal cord, which rapidly led to progressive tetraparesis. Although the diagnosis was difficult, MRI and CT images helped determine the prognosis. To our knowledge, this is the first case report of canine HS with direct spinal cord involvement associated with spinal necrosis.

Acknowledgments

The authors thank all clinical staff and the laboratory members.

Conflict of interest

The authors declare that there is no conflict of interest.

Authors' contributions

YN and MN were the main contributors in taking care of this patient. YN wrote the manuscript. MN, KI, TI, HH, HS, and KT performed examinations, biopsies, and produced the images. MS and MM performed the necropsy and histological exam and contributed to their descriptions. All authors discussed this patient and approved this manuscript.

References

- Affolter, V.K. and Moore, P.F. 2002. Localized and disseminated histiocytocytic sarcoma of dendritic cell origin in dogs. *Vet. Pathol.* 39, 74–83.
- Dervisis, N.G., Kiupel, M., Qin, Q. and Cesario, L. 2017. Clinical prognostic factors in canine histiocytic sarcoma. *Vet. Comp. Oncol.* 15, 1171–1180.
- Fulmer, A.K. and Mauldin, G.E. 2007. Canine histiocytic neoplasia: an overview. *Can. Vet. J.* 48, 1041–1043, 1046.
- Ishikawa, C., Ito, D., Kitagawa, M. and Watari, T. 2016. Comparison of conventional magnetic resonance

- imaging and nonenhanced three dimensional time-of-flight magnetic resonance angiography findings between dogs with meningioma and dogs with intracranial histiocytic sarcoma: 19 cases (2010-2014). *J. Am. Vet. Med. Assoc.* 248, 1139–1147.
- Mariani, C.L., Jennings, M.K., Olby, N.J., Borst, L.B., Brown, Jr J.C., Robertson, I.D., Seiler, G.S. and MacKillop, E. 2015. Histiocytic sarcoma with central nervous system involvement in dogs: 19 cases (2006-2012). *J. Vet. Intern. Med.* 29, 607–613
- Ogawa, K., Akimoto, T., Hara, M., Morita, A., Fujishiro, M., Suzuki, Y., Soma, M., Kamei, S. and Nakajima, H. 2019. Clinical study of thirteen patients with spinal cord infarction. *J. Stroke Cerebrovasc. Dis.* 28, 104418.
- Secrest, S. and Sakamoto, K. 2014. Halo and reverse halo signs in canine pulmonary computed tomography. *Vet. Radiol. Ultrasound* 55, 272–277.
- Song, R.B., Vite, C.H., Bradley, C.W. and Cross, J.R. 2013. Postmortem evaluation of 435 cases of intracranial neoplasia in dogs and relationship of neoplasm with breed, age, and body weight. *J. Vet. Intern. Med.* 27, 1143–1152.
- Tamura, S., Tamura, Y., Nakamoto, Y., Ozawa, T. and Uchida, K. 2009. MR imaging of histiocytic sarcoma of the canine brain. *Vet. Radiol. Ultrasound* 50, 178–181.
- Taylor, A., Eichelberger, B., Hodo, C., Cooper, J. and Porter, B. 2015. Imaging diagnosis-spinal cord histiocytic sarcoma in a dog. *Vet. Radiol. Ultrasound* 56, E17-E20.
- Thongtharb, A., Uchida, K., Chambers, J.K., Kagawa, Y. and Nakayama, H. 2016. Histological and immunohistochemical studies on primary intracranial canine histiocytic sarcomas. *J. Vet. Med. Sci.* 78, 593–599.
- Toyoda, I., Vernau, W., Sturges, B.K., Vernau, K.M., Rossmesl, J., Zimmerman, K., Crowe, C.M., Woolard, K., Giuffrida, M., Higgins, R.J. and Dickinson, P.J. 2020. Clinicopathological characteristics of histiocytic sarcoma affecting the central nervous system in dogs. *J. Vet. Intern. Med.* 34, 828–837.
- Wada, M., Hasegawa, D., Hamamoto, Y., Yu, Y., Fujiwara-Igarashi, A. and Fujita, M. 2017. Comparisons among MRI signs, apparent diffusion coefficient, and fractional anisotropy in dogs with a solitary intracranial meningioma or histiocytic sarcoma. *Vet. Radiol. Ultrasound* 58, 422–432.
- Yasui, H., Ozawa, N., Mikami, S., Shimizu, K., Hatta, T., Makino, N., Fukushima, M., Baba, S. and Makino, Y. 2017. Spinal cord ischemia secondary to epidural metastasis from small cell lung carcinoma. *Am. J. Case Rep.* 18, 276–280.